

Supercontinuum pulse measurement by molecular alignment based cross-correlation frequency resolved optical gating

Jia Liu,¹ Yahui Feng,¹ Hao Li,¹ Peifen Lu,¹ Haifeng Pan, Jian Wu,^{1,2} and Heping Zeng^{1,*}

¹State Key Laboratory of Precision Spectroscopy, East China Normal University, Shanghai 200062, China

²jwu@phy.ecnu.edu.cn

*hpzeng@phy.ecnu.edu.cn

Abstract: We demonstrate that complex supercontinuum and few-cycle ultrashort laser pulses can be fully characterized by using a cross-correlation frequency-resolved optical gating with molecular alignment induced birefringence functioned as a gate. The temporal envelope and phase of the broadband supercontinuum pulse are retrieved by the principal component generalized projection algorithm. This technique shows advantages without phase-matching constraint that may limit the measurable spectral bandwidth, experimental robustness in operating through the whole transparent spectral region of the molecular gases, and intensity sensitivity to measure weak pulses which is inherited from the intrinsic linear process in recording the molecular birefringence induced polarization spectroscopy. Experimental measurements of a few-cycle pulse in the visible region of 525–725 nm confirm that the molecular alignment gating supports a full field characterization of the ultrashort pulse around 10 fs in duration.

©2010 Optical Society of America

OCIS codes: (320.7100) Ultrafast measurements; (190.7110) Ultrafast nonlinear optics.

References and links

1. A. Couairon, M. Franco, A. Mysyrowicz, J. Biegert, and U. Keller, "Pulse self-compression to the single-cycle limit by filamentation in a gas with a pressure gradient," *Opt. Lett.* **30**(19), 2657–2659 (2005).
2. J. Yu, D. Mondelain, G. Ange, R. Volk, S. Niedermeier, J. P. Wolf, J. Kasparian, and R. Sauerbrey, "Backward supercontinuum emission from a filament generated by ultrashort laser pulses in air," *Opt. Lett.* **26**(8), 533–535 (2001).
3. I. Hartl, X. D. Li, C. Chudoba, R. K. Ghanta, T. H. Ko, J. G. Fujimoto, J. K. Ranka, and R. S. Windeler, "Ultrahigh-resolution optical coherence tomography using continuum generation in an air-silica microstructure optical fiber," *Opt. Lett.* **26**(9), 608–610 (2001).
4. X. Gu, L. Xu, M. Kimmel, E. Zeek, P. O'Shea, A. P. Shreenath, R. Trebino, and R. S. Windeler, "Frequency-resolved optical gating and single-shot spectral measurements reveal fine structure in microstructure-fiber continuum," *Opt. Lett.* **27**(13), 1174–1176 (2002).
5. P. Lu, J. Liu, H. Li, H. Pan, J. Wu, and H. Zeng, "Cross-correlation frequency-resolved optical gating by molecular alignment for ultraviolet femtosecond pulse measurement," *Appl. Phys. Lett.* **97**(6), 061101 (2010).
6. H. Stapelfeldt, and T. Seideman, "Colloquium: Aligning molecules with strong laser pulses," *Rev. Mod. Phys.* **75**(2), 543–557 (2003).
7. R. Weigand, J. T. Mendonça, and H. M. Crespo, "Cascaded nondegenerate four-wave-mixing technique for high-power single-cycle pulse synthesis in the visible and ultraviolet ranges," *Phys. Rev. A* **79**(6), 063838 (2009).
8. V. Renard, M. Renard, S. Guérin, Y. T. Pashayan, B. Lavorel, O. Faucher, and H. R. Jauslin, "Postpulse molecular alignment measured by a weak field polarization technique," *Phys. Rev. Lett.* **90**(15), 153601 (2003).
9. J. Wu, H. Cai, Y. Tong, and H. Zeng, "Measurement of field-free molecular alignment by cross-defocusing assisted polarization spectroscopy," *Opt. Express* **17**(18), 16300–16305 (2009).
10. J. Itatani, J. Levesque, D. Zeidler, H. Niikura, H. Pépin, J. C. Kieffer, P. B. Corkum, and D. M. Villeneuve, "Tomographic imaging of molecular orbitals," *Nature* **432**(7019), 867–871 (2004).
11. R. Velotta, N. Hay, M. B. Mason, M. Castillejo, and J. P. Marangos, "High-order harmonic generation in aligned molecules," *Phys. Rev. Lett.* **87**(18), 183901 (2001).
12. T. Kanai, S. Minemoto, and H. Sakai, "Quantum interference during high-order harmonic generation from aligned molecules," *Nature* **435**(7041), 470–474 (2005).

13. S. Varma, Y.-H. Chen, and H. M. Milchberg, "Trapping and destruction of long-range high-intensity optical filaments by molecular quantum wakes in air," *Phys. Rev. Lett.* **101**(20), 205001 (2008).
 14. H. Cai, J. Wu, X. Bai, H. Pan, and H. Zeng, "Molecular-alignment-assisted high-energy supercontinuum pulse generation in air," *Opt. Lett.* **35**(1), 49–51 (2010).
 15. J. Wu, Y. Tong, X. Yang, H. Cai, P. Lu, H. Pan, and H. Zeng, "Interaction of two parallel femtosecond filaments at different wavelengths in air," *Opt. Lett.* **34**(20), 3211–3213 (2009).
 16. H. Cai, J. Wu, H. Li, X. Bai, and H. Zeng, "Elongation of femtosecond filament by molecular alignment in air," *Opt. Express* **17**(23), 21060–21065 (2009).
 17. J. Wu, P. Lu, J. Liu, H. Li, H. Pan, and H. Zeng, "Ultrafast optical imaging by molecular wakes," *Appl. Phys. Lett.* **97**(16), 161106 (2010).
 18. P. B. Corkum, C. Rolland, and T. Srinivasan-Rao, "Supercontinuum generation in gases," *Phys. Rev. Lett.* **57**(18), 2268–2271 (1986).
 19. R. Trebino, K. W. DeLong, D. N. Fittinghoff, J. N. Sweetser, M. A. Krumbügel, B. A. Richman, and D. J. Kane, "Measuring ultrashort laser pulses in the time-frequency domain using frequency-resolved optical gating," *Rev. Sci. Instrum.* **68**(9), 3277 (1997).
 20. D. J. Kane, and R. Trebino, "Single-shot measurement of the intensity and phase of an arbitrary ultrashort pulse by using frequency-resolved optical gating," *Opt. Lett.* **18**(10), 823–825 (1993).
 21. K. W. De Long, D. N. Fittinghoff, R. Trebino, B. Kohler, and K. Wilson, "Pulse retrieval in frequency-resolved optical gating based on the method of generalized projections," *Opt. Lett.* **19**(24), 2152–2154 (1994).
 22. J. Wu, H. Cai, P. Lu, X. Bai, L. Ding, and H. Zeng, "Intense ultrafast light kick by rotational Raman wake in atmosphere," *Appl. Phys. Lett.* **95**(22), 221502 (2009).
 23. C. Marceau, Y. Chen, F. Théberge, M. Châteauneuf, J. Dubois, and S. L. Chin, "Ultrafast birefringence induced by a femtosecond laser filament in gases," *Opt. Lett.* **34**(9), 1417–1419 (2009).
 24. A. Baltuška, M. S. Pshenichnikov, and D. A. Wiersma, "Amplitude and phase characterization of 4.5-fs pulses by frequency-resolved optical gating," *Opt. Lett.* **23**(18), 1474–1476 (1998).
 25. S. Akturk, C. D'Amico, and A. Mysyrowicz, "Measuring ultrashort pulses in the single-cycle regime using frequency-resolved optical gating," *J. Opt. Soc. Am. B* **25**(6), A63 (2008).
 26. Z. Wang, E. Zeek, R. Trebino, and P. Kvam, "Determining error bars in measurements of ultrashort laser pulses," *J. Opt. Soc. Am. B* **20**(11), 2400 (2003).
 27. K. W. DeLong, R. Trebino, and W. E. White, "Simultaneous recovery of two ultrashort laser pulses from a single spectrogram," *J. Opt. Soc. Am. B* **12**(12), 2463 (1995).
 28. W. H. Press, W. T. Vetterling, S. A. Teukolsky, and B. R. Flannery, *Numerical Recipes in FORTRAN: the Art of Scientific Computing*, 2nd ed. (Cambridge U. Press, Cambridge, 1992).
-

1. Introduction

The study of super-continuum (SC) generation by femtosecond laser pulses has attracted much attention for extensive applications in the fields including few-cycle pulse compression [1], remote sensing [2], and time-resolved spectroscopy and coherent tomography [3]. Broadband SC pulse generation normally involves a lot of nonlinear processes such as self-phase modulation, four-wave mixing, stimulated Raman scattering, self-steepening, and material intrinsic dispersions, which inevitably bring about complex phase and temporal structures. So far, it is still a challenge to fully characterize an ultra-broadband SC pulse of weak field intensity, mainly due to the broadband phase matching constraint. By using sum-frequency generation based cross-correlation frequency resolved optical gating (XFROG), SC pulse measurement was demonstrated [4] where the broadband phase-matching between the SC and pump pulses was achieved by angle-dithering a thin nonlinear crystal.

In this paper, we demonstrate that complex SC pulses can be fully characterized by using molecular alignment based cross-correlation polarization-gating frequency resolved optical gating (M-XFROG) [5], where the impulsive molecular alignment induced molecular birefringence is used as the gate function. In principle, the M-XFROG exhibits exceptional features as follows. (i) As long as there is a nonlinear frequency mixing process, the phase matching condition must be considered. However, M-XFROG requires no phase-matching and thus the whole SC spectrum can be measured as long as it lies in the transparent spectral range of the molecular gas. So the limitation of the measurable spectral bandwidth due to phase matching is not a main obstacle. (ii) Although the molecular alignment itself is a nonlinear process whose degree is proportional to the pump pulse intensity, the transient birefringence induced polarization variation of the target pulse is actually linear. By recording such linear polarization variation, M-XFROG can be potentially used to measure weak field intensity with

optimized experimental condition. (iii) Crystals introduce relatively large distortion even though the dispersion is not a big issue when an ultrathin crystal is used. For example, the group velocity dispersion (GVD) induced by a 150 μm thick SHG BBO (type I) at 800 nm is calculated to be $\sim 11.2 \text{ fs}^2$, which is equivalent to a $\sim 2.8 \text{ m}$ long CO_2 gas we used in the experiment. So the low dispersion of the gaseous molecules induces quite small distortion to the target pulse that enables us to retrieve the original information of it. (iv) The gate induced by molecular alignment is insensitive to the slight fluctuation of the excitation pulse, since it is based on the quantum beating among the pre-populated rotational wavepackets. Moreover, the gate function, originated from the transient birefringence, is a “real” quantity as it does not contain any phase information. (v) The experimental implementation of M-XFROG is quite convenient in molecular gas (e.g. air), and the recorded wavelengths are indeed those of the target pulse. M-XFROG hence can work as a convenient and robust tool for full characterization of the complex broadband SC pulse.

Linear molecules can be aligned along the field polarization by impulsive rotational Raman excitation with ultrashort laser pulses, and the molecular alignment experiences periodic revivals after the extinction of the pump pulse [6]. The pre-aligned molecules show orientation-dependent refractive index changes as $\delta n = 0.5(\rho_0 \Delta\alpha/n_0)(\langle\langle \cos^2\theta \rangle\rangle - 1/3)$, where ρ_0 is the initial molecule density, $\Delta\alpha = \alpha_{\parallel} - \alpha_{\perp}$ is the polarizability difference between the components parallel and perpendicular to the molecular axis, n_0 is the linear refractive index of the randomly orientated molecules. The molecular alignment degree is characterized by the metric $\langle\langle \cos^2\theta \rangle\rangle$, which is greater, less, and equal to 1/3 for parallel, perpendicular, and random molecular alignments, respectively. Here, θ is the angle between the field polarization of the pump pulse and molecular axis. The polarization modulation based M-XFROG is similar to the cross-correlation polarization-gating FROG in bulk media, which was recently used for full characterization of the multicolored femtosecond pulses [7]. For the M-XFROG presented here, laser pulses propagating through the pre-aligned molecules experience a respectively increased and decreased refractive index for the field components parallel and perpendicular to the molecular alignment, leading to different phase velocities between the orthogonally polarized field components. The polarization mode of the laser pulse is hence changed by this molecular alignment induced birefringence, which essentially works as a transient wave-plate. For a linearly polarized laser pulse, such polarization modulation can be analyzed after an orthogonally aligned polarizer, which composes the polarization spectroscopy technique and has been used for molecular alignment measurements [8,9]. Here, we use this molecular alignment induced transient birefringence as the gate function for FROG measurement to characterize the complex SC pulses. The width of the molecular alignment induced gate is determined by the bandwidth of the excitation pulse, molecular gas temperature and species. Actually, impulsive molecular alignment has been extensively used for molecular orbital reconstruction [10], high harmonic generation [11,12], dynamic control of intense laser propagations [13–16], and very recently for ultrafast optical imaging [17].

2. Experimental setup

To demonstrate the capability of M-XFROG for SC pulse measurement, we performed experiments as schematically illustrated in Fig. 1(a). The output from an amplified Ti:sapphire laser system ($\sim 35 \text{ fs}$, 800 nm, 1 kHz) was split into two pulses: one as the aligning pulse for molecular alignment (M-pulse) and the other was used for SC pulse generation. After an iris, the probe pulse was focused into a gas cell filled with atomic Xe at a pressure of 2 atm [18] by a convex lens of $f=20 \text{ cm}$, which generated stable broadband SC pulse with an optimal iris aperture size. The M-pulse was down-collimated before it was sent to cross with the SC pulse in the second gas cell filled with molecular CO_2 , so that a large interaction region could be resulted. The polarization of the M-pulse was rotated to be 45° by a half-wave plate (HWP2) with respect to the SC pulse, whose pulse energy could be tuned by adjusting the half-wave plate (HWP1) before the thin film polarizer. The polarization modulated spectrum of the SC

pulse was measured by a spectrometer (HR4000, Ocean Optics) with a spectral resolution of 0.27 nm after a Glan prism (GP) (extinction ratio $\sim 1:10^{-6}$) whose transmission direction was orthogonal to the polarization of the incident SC pulse. Therefore, only the field components whose polarizations were rotated by the molecular alignment induced transient birefringence were recorded by the spectrometer after the polarizer. The transmitted spectra of the SC pulse were measured as its time delay with respect to the M-pulse, which formed the XFROG trace. In order to increase the signal-to-noises ratio, each spectrum at a certain time delay was averaged for ten times to produce an M-XFROG trace. Moreover, a mean background subtraction was applied in the retrieval algorithm allowed us to further reduce the background. The measured XFROG trace had dimensions of 3648×512 , which was interpolated and expanded to 1024×1024 for temporal envelope and phase retrieval. In these demonstrations, the pulse energies of the M-pulse and the generated SC pulse were measured to be $\sim 800 \mu\text{J}$ and $70 \mu\text{J}$, respectively, which were crossed with an angle of $\sim 4^\circ$ in the CO_2 gas cell.

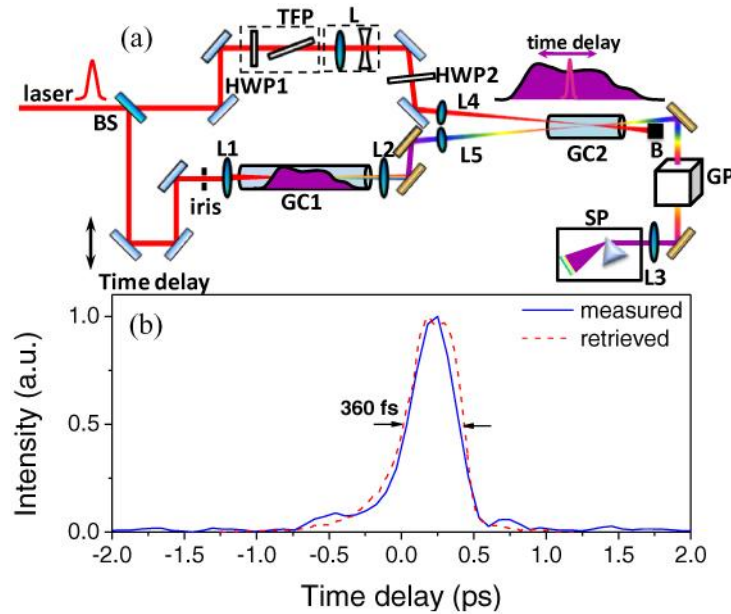


Fig. 1. (a) Schematic configuration of the experiment setup. BS: beam splitter; HWP1, HWP2: half-wave plate at 800 nm; TFP: thin film polarizer; GC1: Xe gas cell; GC2: CO_2 gas cell; GP: polarizer; SP: spectrometer; (b) Measured CO_2 alignment signal versus the time delay. The red-dashed curve is the retrieved gate with a FWHM of ~ 360 fs, which shows a well accordance to the measured one.

3. Results and discussions

The complex envelope and the phase information of the SC pulse $E(t)=I(t)^{1/2}\exp[-i\phi(t)]$ can be uniquely retrieved from the measured spectrogram, which is numerically given by [19,20]

$$I(\omega, \tau) = \left| \int_{-\infty}^{+\infty} E(t)G(t-\tau)e^{-i\omega t} dt \right|^2. \quad (1)$$

Here, $G(t-\tau)$ is the transient molecular alignment induced gate function. The conventional XFROG pulse retrieval algorithms, based on the iterative Fourier transformation and the principle component generalized projections algorithm, were used for the SC pulse retrieval [21]. Figure 1(b) shows the measured molecular alignment signal of molecular CO_2 by using ultrashort 35-fs laser pulses. The CO_2 molecules were impulsively aligned shortly after the excitation pulse, and then field-free revived due to the quantum beatings of the excited

molecular rotational wave-packets. In principle, any of the molecular alignment revivals can be used as the gate function. Here we used the molecular alignment of CO₂ shortly after the zero time delay (~180 fs after the excitation laser pulse) as the gate function for its clear and simple single-peak structure, whose gate width was measured to be 360 fs as shown in the Fig. 1(b). The contribution of the instantaneous Kerr effect during the pulse duration to the gate function was small as compared with the molecular alignment effect [22,23]. This was confirmed in our experiments and will be discussed elsewhere in detail.

Since our measurements were performed for a noncollinear scheme, the time smearing effect should also be included. In our experiments for a crossing angle of $\theta=4^\circ$, the time smearing δt was estimated to be ~0.6 fs. Moreover, Similar to the frequency response of the nonlinear frequency mixing process for the FROG as discussed in Ref [24,25], a reliable measurement requires extremely careful concerning about the wavelength response of the whole involved optical components owing to the broadband frequencies of the SC pulse. The wavelength response, acquired by compare the directly measured spectrum of the SC pulse (blue-squared curve) and the time marginal of the M-XFROG trace (red-circular curve), is shown in Fig. 2(a). Such wavelength calibration was implemented to the measured FROG in the retrieval process to get the real time and frequency resolved spectrogram.

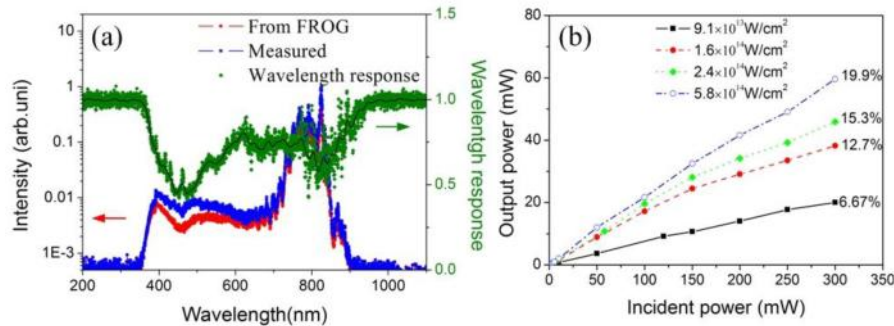


Fig. 2. (a) The wavelength response of the M-XFROG apparatus (olive-scattered dot). (b) The polarization modulated pulse power variation as a function of incident pulse power under different excitation intensities.

The modulation efficiency is defined as the ratio of the polarization rotated pulse energy to that of the whole incident pulse. Such modulation depth is correlated to the molecular alignment induced birefringence, which is determined by the molecular gas, the excitation pulse energy and temperature. Figure 2(b) shows the polarization modulated pulse power variation as a function of incident pulse power under different excitation pulse intensities for room-temperature air, whose slopes account for the modulation efficiency. A nearly linear response to the incident power is evidently illustrated, and the modulation efficiency is increased along with the increased excitation pulse intensity. The M-XFROG is operated by recording a linear process of polarization variation induced by molecular alignment and is potentially able to measure very weak pulses. However, there must be a limit of the lowest power that can be resolved in the practical experiment apparatus. Here, by considering the spectrometer sensitivity (~100 photons/count), the transmittance of the optical component (~50%), the extinction ratio of the polarizer (~10⁻⁶), and the modulation efficiency, the sensitivity is estimated to be several nJ. We experimentally confirmed a measurement of input pulse energy as low as ~300 nJ due to the limitation of the power-meter used in our measurements. High sensitivity is expected with optimized spectrometer, optical components and high-degree molecular alignment.

The calibrated spectrogram of the SC pulse over a time delay range of ~3 ps is plotted in Fig. 3(a). The lower frequency components are advancing as compared with the higher ones, implying a positive chirp structure of the generated SC pulse. Figure 3(b) shows the retrieved

spectrogram for an M-XFROG trace error of 0.01% after 400 iterations. The retrieved intensity and phase structures of the SC pulse are shown in Fig. 3(c), with error bars obtained using the bootstrap method [26], which has picosecond pulse duration and split into several sub-pulses. The quadratic phase clearly indicates the positive chirp structure of the SC pulse as implied by the XFROG trace. As shown in Fig. 3(d), apart from some minor difference, the overall shape and peak positions of the measured (red-solid curve) and reconstructed spectra (black-dashed curve) agree well with each other, the SC spectrum before wavelength calibration (olive-dashed dotted curve) is also depicted in Fig. 3(d) as a comparison.

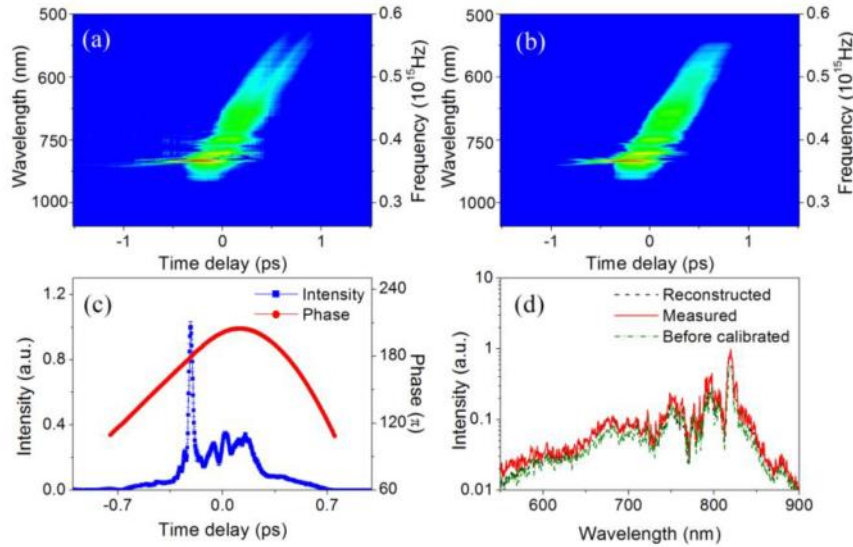


Fig. 3. (a) The measured M-XFROG trace. (b) The retrieved M-XFROG trace of the SC pulse. (c) The retrieved SC intensity (blue-squared curve) and phase (red-circular curve) as a function of time. (d) The reconstructed (black-dashed curve) and the measured (black-solid curve) spectrum in Log scale.

To confirm the correction of the molecular alignment induced gate function for the measured M-XFROG spectrogram and the reliability of the retrieval process discussed above, we used the twin retrieval of excitation electric fields frequency-resolved optical gating (TREEFROG) algorithm [27] to simultaneously reconstruct the gate and target pulses. In each generalized projection, both the target pulse $E(t)$ and gate function $G(t)$ are generated by using the singular value decomposition method from the cross-correlation signal $E'_{sig}(t, \tau)$ [28]. As shown in Fig. 1(b), the retrieved gate function by the TREEFROG algorithm agrees well with the measured molecular alignment signal, indicating the reliability of our M-XFROG for the complex SC pulse characterization. As compared with the TREEFROG, the M-XFROG with well-known gate function is more robust against the noise or fluctuation of the experimental measurements. The width of the molecular alignment induced gate function is determined by the number of the coherently coupled rotational wavepackets since it results from the quantum beating of them. In general, a narrow molecular alignment gate function is expected when a broadband excitation pulse and higher temperature molecular gases were used.

The M-XFROG can be not only used to characterize the complex long pulse, but also versatile for diagnosis of ultrashort laser pulses in various spectral regions. A stable single-core high-energy SC pulse of ~ 2.5 mJ was generated by focusing the input fs pulse into a 1.2 m long gas tube filled with 0.3 atm Xe and 0.7 atm air, which was then compressed by using two pairs of chirped mirrors. The measured and retrieved M-XFROG traces for the spectral range from 525 to 725 nm are shown in Figs. 4(a) and 4(b), respectively. Figure 4(c) illustrates the retrieved temporal profile and phase of the SC pulse, with error bars obtained using the bootstrap method

[26], which indicates a few-cycle pulse with a duration of 12.8 fs (FWHM). The maximum signal-to-noise ratio of the traces is about ~ 700 . The spectrum reconstructed by Fourier transforming the retrieved pulse temporal envelope is represented in Fig. 4(d) (black-dashed curve), which shows almost perfect agreement with the measured one (red-solid curve). Although the width of the molecular alignment gate function we used here was much longer than that of the ultrashort pulse, the result presented here strongly demonstrated that the M-XFROG could be used in such ultrashort circumstances. This was benefited from the cross-correlation essential of the M-XFROG, where the ultrashort target pulse was used to scan the relatively long molecular alignment gate. We confirmed with numerical simulations that the M-XFROG is estimated to be applied to diagnose pulse with its pulse duration not less than 3 fs at the current experimental condition. However, this value will be reduced if a shorter gate function is used in an optimized experimental condition.

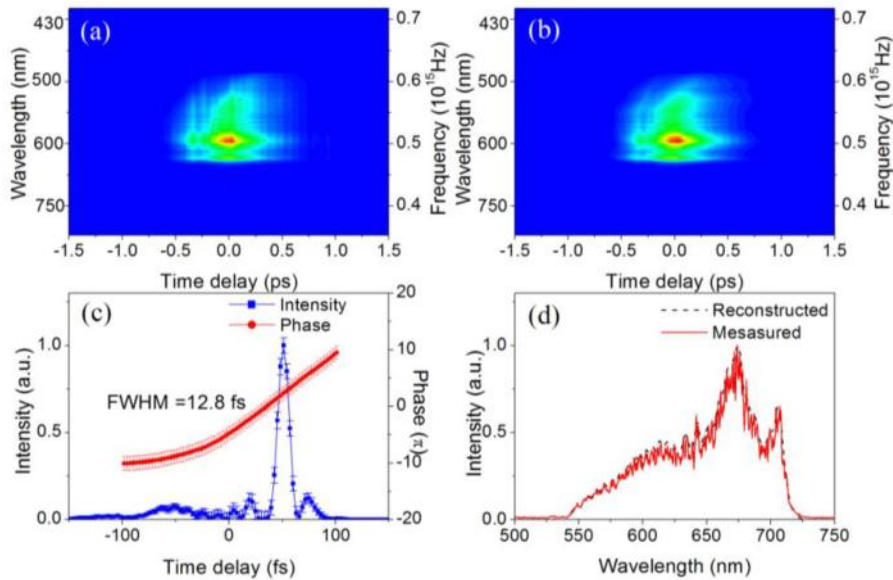


Fig. 4. (a) The measured M-XFROG trace. (b) The retrieved M-XFROG trace of the ultrashort pulse. (c) The retrieved temporal profile (blue-squared curve) and phase (red-circular curve) of the ultrashort pulse, with error bars obtained using the bootstrap method. (d) The reconstructed (black-dashed curve) and the measured (red-solid curve) spectra of the ultrashort pulse.

4. Summary

In summary, we have demonstrated that the M-XFROG could be used to fully characterize the complex SC pulse, which showed great advantages over the nonlinear frequency mixing based XFROG methods. Without the phase-matching constraint, the M-XFROG technique provides us a promising approach for SC pulse measurements, which can be readily extended for other laser pulse measurements where the low intensity or broadband spectral range that the nonlinear frequency mixing based XFROG technique is difficult to handle, such as weak pulses in the ultraviolet spectral region.

Acknowledgement

This work was partly funded by National Natural Science Fund (10525416 and 10804032), National Key Project for Basic Research (2006CB806005), and Projects from Shanghai Science and Technology Commission (08ZR1407100 and 09QA1402000).